IoT-based electromagnetic actuator for CVT: basic design and prototyping

Ataur Rahman*, Abdul Hassan Jaffar and Sany Izan Ihsan

Department of Mechanical Engineering,
Faculty of Engineering,
International Islamic University Malaysia,
50728 KL, Malaysia
Email: arat@iium.edu.my
Email: aseuia@gmail.com
Email: sihsan@iium.edu.my
*Corresponding author

Abstract: Resulting from the slow fluid pressure responses and fluid viscosity loss, the present hydraulic-powered CVTs produce jerky movements, rattling noise and unequal power transmission at uphill climbing. The aim of this article is to present a design and prototyping of an electromagnetic actuated continuously variable transmission (EMA-CVT). Using the kinematics analysis of CVT clamping forces and electromagnetic forces, the EMA-CVT is modelled. An internet of things (IoT) has been developed to control the EMA-CVT gear ration with integrating a fuzzy logic controller CVT, wheel speed sensor, CVT pulley position sensor, and CVT secondary pulley revolution sensor. The fuzzy logic controller is used to control the current supply to the EMA. The CVT has a failsafe mode that allows to manually adjust the gear ratio if any of the sensor of the IoT system malfunctions. The EMA develops the electromagnetic force in the range of 185–266 N for the supply current in the range of 3–3.7 amps.

Keywords: green transportation; electromagnetic actuator; EMA; IoT-based controller; CVT; energy efficient.

Reference to this paper should be made as follows: Rahman, A., Jaffar, A.H. and Ihsan, S.I. (2022) 'IoT-based electromagnetic actuator for CVT: basic design and prototyping', *Int. J. Powertrains*, Vol. 11, No. 1, pp.38–61.

Biographical notes: Ataur Rahman is a Professor at the Department of Mechanical Engineering, International Islamic University Malaysia (IIUM), in 2006. He is the Chairman at the Centre of Excellence of Electric Mobility, IIUM and Chairman, a flagship project, IIUM. He is a Visiting Professor of Military Institute of Science and Technology (MIST), Dhaka, Bangladesh and Visiting Fellow in Mechanical Engineering Laboratory, The University of Tokyo, Japan. His research interests are green transportation system: EV/HEV, intelligent evaporative thermal management system for EV battery, intelligent power train for hybrid and electrical vehicle, intelligent steering system and traction control system, electromagnetic CVT and autonomous electromagnetic two-speed gearbox and organic solar-capacitor for EV. He has published 165 index journal articles, four books and seven patents. He has published three books: *Green Transportation System*, IIUM Press, International Islamic University, Malaysia, and *The Peat Swamp: Productivity and livelihood, Traficability and Mechanization*, Nova Science Publication, Inc., New York, USA.

Abdul Hassan Jaffar obtained his PhD from the Department of Mechanical Engineering, Kulliyyah of Engineering, International Islamic University Malaysia. His research interests are in electromagnetic continuously variable transmission, electromagnetic two speed gear box, IoT-based electric vehicle powertrain innovation, fast charging system for electric vehicle batteries and vehicle autonomous system.

Sany Izan Ihsan is an Associate Professor at the Mechanical Engineering Department, and currently the Dean of Kulliyyah of Engineering, International Islamic University Malaysia (IIUM). He received his BSc in Mechanical Engineering at the University of Wisconsin – Madison in 1995, MSc in Aerospace Engineering at University of Tennessee Space Institute (UTSI) in 1999 and PhD in Engineering from IIUM in 2008. His research areas of interest include noise and vibration, ride quality, vehicle dynamic and control, semiactive control system, solar thermal, renewable energy and engineering education.

1 Background of research

Continuously variable transmissions are built with fewer parts compared to conventional transmissions, they are less expensive to manufacture. This savings is passed along to consumers in a car's selling price. Acceleration stays in a 'sweet spot' to minimise wasted power, thus improving a vehicle's fuel efficiency. In the most advanced form, the CVT and its control form an actuation system for the transmission which determines the best operating speed and torque of the engine given a set of driver inputs and car operating conditions (Kluger and Fussner, 1997; Tawi et al., 2015). Brockbank and Burtt (2007) reported 15% less fuel consumption for the CVT transmission than with a standard gearbox combined with a reduction in harmful emissions of about 30%. A simulation study by Kluger and Fussner (1997) of automated vehicle (AVL) installation, the world's largest private and independent company for the development of hydropower systems with indoor combustion engines compares different CVT concepts with manual transmissions for gasoline and diesel engines and a demonstration of up to 10% less fuel consumption for gasoline engines and 19% for diesel engines. Ang et al. (2002) studied the performance of a 3,000 cc car by simulating manual transmission, automatic transmission, and the continuous variable transmission. They stated that the time taken was 10.20 s for acceleration to 100 km/h for manual transmission, 10.76 s for automatic transmission, 7.85 s for CVT. Toys what CVT acceleration time 11.3 s (0–100 km/h) (Toyota Wish CVT Specifications, 2018). CVT is preferred over other automatic transmission because of some reasons most likely the comfortability, reliability, durability as well as the efficiency (Kelly, 2017; Nogill et al., 2009; Pesgens et al., 2006). The power flow through the power train does not need to be interrupted during acceleration as in conventional transmissions and this makes it possible to gain a smooth, rapid and steeples response to drivers' demand without disturbing jerk. Technically, oil hydraulic system is preferred over the pneumatic due to leakage and compressible fluid when high accuracy and a great amount of pressure are needed (Nissan Technological Development Activities Overview: Xtronic Cvt, 2012; Rahman et al., 2012b; Tanaka and Machida, 1996). Pesgens et al. (2006) studied on the hydraulic control (housing system)

high gear and low gear mechanism for CVT and it was reported that the system is quite effective to develop the sufficient pressure but the problem is to hold the movable sheave of the pulley as it is desired. Though spring can be used, owing to spring oscillation there will be a slip, which results in torque losses.

Fluid pump loss is one of the major sources of torque loss in modern CVT. The toroidal half CVT could not replace because of its large contact component leading to an imperfect contact angle (Rahman et al., 2014b). This problem was exacerbated by the comparative delay control strategies that allowed engine speed to reach its maximum speed range after full pedal insertion and only after a delay did the engine speed increase. The study of the electromagnetic actuator (EMA) was performed for the fast and smooth operation of the rotary pulley rotor to adjust the desired gear ratio to meet the vehicle torque-velocity demand (Boldea and Nasar, 1997; Leander et al., 1987; Toshie, 2004). The power supply control of an EMA has been adjusted to maintain the instantaneous gear ratio of the CVT (Toshie et al., 2004; Sharif et al., 2013).

The authors (Boldea and Nasar, 1997; Nissan, 2017) have developed a plastic housing electromagnetic bobbin actuator for the CVT system. They have reported that the performance of the plastic-bobbin EMA is high efficient but lot of power loses due to the heat. The temperature was recorded of the EMA at 80C which caused the plastic bobbin about to melt due to the current supply in the range of 10–12 A to the EMA, which can cause the plunger to be grasped (Boldea and Nasar, 1997; Leander et al., 1987; Toshie, 2004). They have also reported that the plastic-bobbin housing has numerous problems such as holding electromagnetic energy flux and shape of the structure of the bobbin.

The objective of this manuscript is to present an EMA for the actuation of the CVT to maintain the various gear-ratio of the powertrain. In prototyping of the EMA, the design analysis work was carried out, including the gear ratio of the transmission, vehicle torque requirements, transmission parameters and the conceptual design of the gearbox, including automatic operation associating the design of electromagnetic solenoid. The researchers have tested the feasibility of the EMA prototype with a CVT both in acceleration and cruising. The automatic system was used to control by an IoT-based fuzzy logic controller (FLC) to control the battery power flow to the EMA. The controller controls the flow of current to the EMA based on the output of the load cell and the RPM sensor (Boldea and Nasar, 1997; Sharif et al., 2013; Rahman et al., 2014a).

2 Methodology

This section presents simplified mathematical models for the development of EMA, based on the requirements of the maximum load of the car; a fuzzy logic expert system (FLES) to monitor the dynamic behaviour of the EMACVT; and an experimental EMA-CVT performance study model with our developed test-rig. This section also presents an analytical model of the principle of EMA operation while maintaining a nonlinear characteristic of clamping force with developing electromagnetic force at any vehicle loads, followed by a computational and mathematical approach. This section also introduces the lab-scale EMA-CVT for exploring the development of a full-blown EMA-CVT for a passenger car.

2.1 EMA-CVT modelling

The clamping force F_c is the force that exit from the actuation force of the primary pulley. It is assumed that a spring is used for producing the primary and secondary pulley actuation force (Figure 1), F_c which is called the clamping force for each of the pulleys and it is estimated as $F_c(t) = k_s\delta_p(t)$ where k_s is the spring stiffness that keeps the primary pulley in the highest diameter in N/mm and $\delta_p(t)$ is the instantaneous displacement. In this study, we have replaced the spring of the secondary spring by an EMA. In order to change the gear ratio of the EMA-CVT, the EMA needs to develop the electromagnetic force, which must be, $F_{em}(t) \geq k_s\delta_s(t)$ for the changing the gear ratio of the CVT to make the vehicle in traction mode or in cruising mode.

Figure 1 Force on CVT pulley surface (see online version for colours)

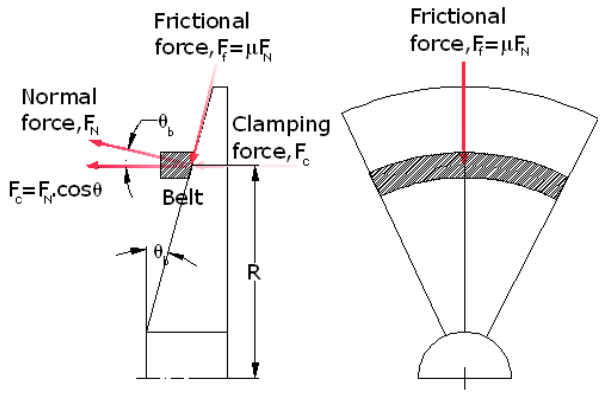

Source: Rahman et al. (2014b) and Boldea and Nasar (1997)

The actuator should be designed in such a way that it will be able to produce electromagnetic force, which is equal or more than the clamping force of the CVT, $F_{em}(t) \geq F_c(t)$ for changing the gear ratio in the range of $0.85 < GR \geq 5$.

The required gear ratio of the vehicle is estimated by using the equation:

$$T_{initial} = m_c g \left[\mu_R \frac{\left(l_f - f_r h\right) \Big/ L_w}{1 + \mu_R h \Big/ L_w} + \sin\theta_R \right] (r_w) \tag{1}$$

$$T_{final} = \left(f_r w + \frac{1}{2} \rho_a A_f C_D v_c^2 \right) r_w \tag{2}$$

By using a car of mass (m_c) of 1,700 kg, maximum speed of 120 km/h or 33 m/s, the road friction coefficient (μ_R) equal to 0.5, the wheel radius (r_w) of 0.295 m, the drag area (C_DA_f) of 0.633, and rolling motion resistance coefficient (f_r) of 0.02. The traction torque (wheel torque, T_w) is calculated by using equation (4) for initial and equation (5) for gradient 30% to be 1,560 Nm and 1,500 Nm respectively (Wong, 2001; Rahman et al., 2012a; Richard et al., 2019).

By considering the CVT gear ratio, the maximum output torque of the secondary pulley is estimated as 390 Nm by considering the final drive ratio 4:1. Based on the input pulley torque, the amount of clamping force required to maintain the pulley sheave at

correct position for the desired gear ratio. The clamping force on the secondary can be estimated as, $F_{c(s)} = k_s\delta_p(t)cos\theta_b$. It is considered that the pulley belt angle (θ_b) is 12°. The clamping force of CVT is 210 N for the maximum gear ratio of 5. The displacement of the spring of the primary pulley is considered 18 mm and the k_s is considered as 11.72 N/mm. Therefore, the EMA needs to develop the actuation force 300 N including its supporting spring force for smooth operation and car fast acceleration. The actuation system of the EMA including the secondary pulley back spring force needs to develop to maintain the torque 390 Nm at the secondary pulley for getting the vehicle traction torque of 1,560 Nm at gear ratio of 5.0.

The CVT's actuation system has been made with the EMA, plunger (one end is connected with the movable sheave of the pulley and the other end with metal disc), a set of springs and power pack. The detail discussion has been made in Section 3. The back spring (EMA's supportive spring) of stiffness 5.86 N/mm has been used to support the EMA to reach the maximum gear ratio of the pulley sets and avoid creep motion during return. The back spring force is estimated as 105 N for the displacement of 18 mm to reach the gear ratio 5. Therefore, the EMA has been developed in this study to produce actuation force of 200 N for the smooth operation of the CVT. However, the primary pulley in this CVT system has a spring of stiffness 11.72 N/mm is used for the actuation of the primary pulley when the power is supplied to the EMA decreased or stop. This operation is considered for the cruising of the vehicle with the gear ratio closed to 1.0. Total actuating force of the EMA including the spring force can be estimated as, $F_{act.} = F_{em} + k_s\partial_s$ where F_{em} is the electromagnetic force in N, k_s is the spring stiffness in N/m, ∂_s is the spring displacement in m.

Figure 2 3D EMA drawing isometric view cut-section view (see online version for colours)

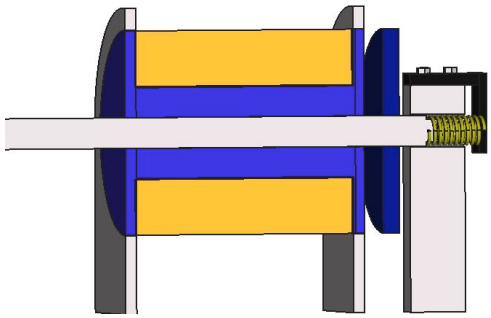

Figure 2 shows the cutting view of EMA for the actuation of CVT. The basic principle of the EMA actuation is incorporated with the DC power supply. When the power is supplied to EMA, the EMA turns to electromagnet and attract the metal disc towards the EMA and the other end pushes movable sheave towards the fixed pulley sheave and set the gear ratio instantly as required. The energy density of EMA for the actuation instantly can be defined as:

$$E_{em}(t) = B^2/2\mu_0 + \varepsilon_0 E^2/2 + \frac{1}{2}k_s x^2 \tag{3}$$

where B is the magnetic field and E is the electric field, k_s is the spring stiffness, kN/m, ε_0 permittivity of free space, ε_0 =8.8542 × $10^{-12}C^2N^{-1}m^{-2}$, μ is the magnetic permeability. A

typical magnetictude of E is considered as 10^6 V.m^{-1} and magnetic permeability about 0.006 H/m.

It is identified that electromagnetic radiation incur during testing of EMA-CVT and it measured based on the changing of temperature around the free surface of the EMA same as we feel hot under in sunlight which is due to the sunlight radiation. Electromagnetic waves are electric and magnetic fields travelling through empty space with the speed of light c (Richard et al., 2019). If its frequency of oscillation is f, then it produces an electromagnetic wave with frequency f. The wavelength λ of this wave is given by $h = c/f$ electromagnetic waves transport energy through space.

The total energy store in the EMA coils due to the supply current can be modelled as:

$$E_{act} = E_{d(EMA)} + E_{sd}$$
$$\text{with } E_{d(EMA)} = \frac{1}{2\mu} B^2 V_{EMA} + \frac{1}{2}\varepsilon_0 E^2 \tag{4}$$

where E_{act} is the energy actuation of the EMA system, $E_{d(EMA)}$ energy develops at the EMA due to supply current, I and E_{sd} developed by the spring and $V_{EMA} = \pi r^2 l_c$ is the volume of the solenoid. If the spring of stiffness k_s is added at the other end of the plunger, by simplifying equation (4), the energy develops by the EMA actuation system can be modelled as:

$$E_{act} = \frac{1}{2}\mu N^2 I^2 V_{EMA} + \frac{1}{2}\varepsilon_0 E^2 + k_s x^2 t_{act} \tag{5}$$

The power loss of the EMA due to the current supplied to its coils $I_0^2 R_{rad}$ associated with the radiation resistance, whereas the power loss $I_0^2 R_c$ associated with the real resistance is due to ohmic heating of the EMA. The R_{rad} can be deified by the equation of Richard et al. (2019) (Denton, 2011):

$$R_{rad} = \frac{2\pi}{3\varepsilon_0 c}\left(\frac{l_c}{\lambda}\right)^2 \tag{6}$$

Total power loss of the EMA can be defined as:

$$P_{EMA(loss)} = I^2\left[R_c + \frac{2\pi}{3\varepsilon_0 c}\left(\frac{l_c}{\lambda}\right)^2\right]$$

The effective energy of the EMA to do the actuation of the CVT's pulley,

$$E_{eff(EMA)} = E_{act(EMA)} - E_{l(oh)} - E_{l(rad)} \tag{7}$$

By simplifying equation (7), the equation can be rewritten as:

$$E_{eff(EMA)} = \frac{1}{2}\mu N^2 I^2 \pi r^2 l_c + \frac{1}{2}\varepsilon_0 E^2 - I^2\left[R_c + \frac{2\pi}{3\varepsilon_0 c}\left(\frac{l_c}{\lambda}\right)^2\right]\int_0^t dt$$

Figure 3 Magnetic flux density of, (a) single coil (b) multiple coils (see online version for colours)

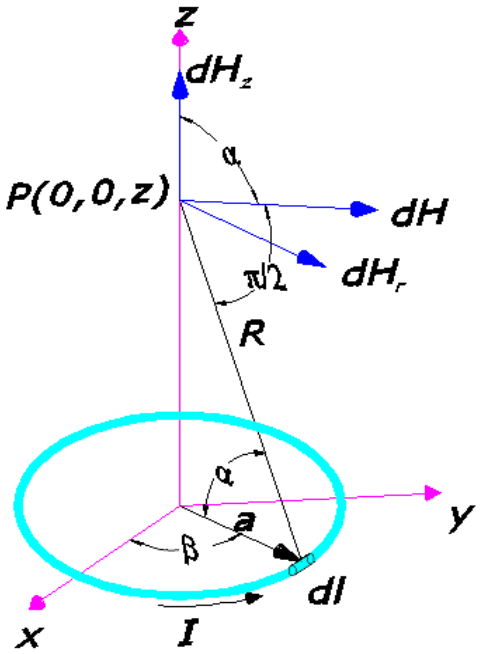

(a)

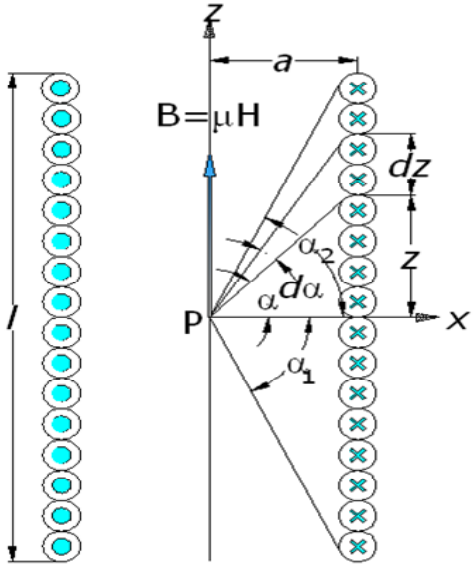

(b)

2.2 EMA force modelling

The EMA has been developed with copper coil winding based on the electromagnetic force (axial shifting force) requirement. Magnetomotive force (MMF) is the equivalent of electro-motive force (EMF or voltage) in an electric circuit. Its units are ampere-turns

(A-t). A coil carrying I amps with N turns generates an MMF of NI ampere-turns. The EMA uses to maintain the gear ratio or the transmission ratio of the vehicle to adjust the gear ratio as required. The battery DC power supply to the EMA has been controlled by a fuzzy controller based on the signal of the sensors. The EMA sets the gear ratio of the CVT automatically based on the response of the sensors (such as slope sensor and speed sensor and/or both).

The electromagnetic force is the function of the magnetic flux density and supply current as the length of the coil pack is considered constant in the magnetic field. By using single coil and multiple coils as shown in Figure 3, the magnetic flux density of EMA can be estimated. The EMA force modelling has been made with simplifying the equations of Gauss's law, Maxwell's equations, ampere circuital equation, Faraday's law and Poynting's equation.

The EMA has considered a thin coaxial cylindrical conducting shells of radii a and c. The current, I is supplied with number of turns N per unit length. According to Gauss's law, the electric field takes the form $E = E_r e_r$ where:

$$E_r = \begin{bmatrix} -Q \big/ (2\pi\varepsilon_0 rl) & \text{for } a \le r \le c \\ 0 & \text{Otherwise} \end{bmatrix} \tag{9}$$

Similarly, according to Ampere's circuital law, the initial magnetic field of the EMA due to supply current:

$$B_z = \begin{bmatrix} \mu_0 NI & \text{for } r \le c \\ 0 & \text{Otherwise} \end{bmatrix} \tag{10}$$

The initial momentum density of the electromagnetic field could be:

$$g_\theta = \begin{bmatrix} \mu_0 NIQ / (2\pi rl) & \text{for } a \le r \le b \\ 0 & \text{Otherwise} \end{bmatrix} \tag{11}$$

Any change in the current flowing in the EMA winding generates an inductive electric field which can be defined as:

$$E_\theta = \begin{bmatrix} -\mu_0 NIr / 2 & \text{for } r \le b \\ -\mu_0 NIb^2 / 2r & \text{Otherwise} \end{bmatrix} \tag{12}$$

However, if a current of uniform density $j = je_z$ within the coil of the EMA, the net energy flux into the EMA surface, coaxial within the wire, of radius r and length l_c could be modelled as, $U = u2\pi rl_c = \rho j^2 V(r)$ where $V_{EMA}(r) = \pi r^2 l_c$ is the volume enclosed by the surface of the EMA and $r = c - a = D_2 - D_1$. The EMA develops the magnetic force; F_{em} is the function of supplied current and number of coils as stated in equation (8). Therefore, the electromagnetic force:

$$F_{em} = \frac{E_{eff(EMA)}}{d} = \frac{1}{d}\left[\frac{1}{2\mu}B^2 V_{EMA} + \frac{1}{2}\varepsilon_0 E^2\right] - I^2\left[\frac{R_c}{l_c} + \frac{R_{rad}}{d(r)}\right] \quad (13)$$

with $B = \mu NI$

d = pulley sheave moval distance, m

where μ is magnetic permeability (degree of magnetisation of a material in response to magnetic field), l_c length of the core, m, $d(r)$ is the distance of the radiation measuring, and t is the time s.

By applying the principle of virtual work, we can model an equation to estimate the total actuation force of the movable sheave of secondary pulley against the clamping force, $F_{c(s)} = k_s\delta_p(t)\cos\theta_b$ as:

$$F_{em} = \frac{1}{d}\left[\frac{1}{2\mu}B^2 V_{ema} + \frac{1}{2}\varepsilon_0 E^2 + k_s\delta_s\right] - I^2\left[\frac{R_c}{l_c} + \frac{R_{rad}}{d(r)}\right]$$

with $B = \mu NI$

d = pulley sheave moval distance, m

where $A_e = \pi\left(\frac{D_2^2 - D_1^2}{4}\right)$ m^2 A_e is the effective cross-sectional area of the EMA.

Normally, it is identified that the current passes to the coil (loop) generates magnetic field. By applying the Ampere's circuital law to an imaginary coil in the x-y plane of radius a, centred in the z-axis as shown in Figure 3(a). The current flows in the coil can be estimated as:

$$I(r) = \begin{cases} 0 & r \le a \\ \left\{I^*(r^2 - a^2)/(c^2 - a^2)\right\} & a \le r \le c \\ I & c > r \end{cases} \quad (14)$$

Hence, the magnetic flux density can be estimated

$$B_\theta(r) = \begin{cases} 0 & r > a \\ \left[\mu I/2\pi r\right]\left[(r^2 - a^2)/(c^2 - a^2)\right] & a \le r \le c \\ \mu I \big/ 2\pi r & c > r \end{cases} \quad (15)$$

Typically, the magnetic permeability μ is considered as 0.006 H/m. It is noted that when the current (I) 17A is supplied to the EMA, EMA's temperature has reached to 100°C, the solenoid efficiency is found 0%. Therefore the energy lost of the EMA as the ohmic heat and electromagnetic radiation as shown in equation (13).

The supply to the EMA to make the vehicle acceleration can be simulated by using the equation, present as follows:

$$a(t) = \begin{vmatrix} At\ start - from - rest & I_{\max} = 12.5\ A \\ At\ G = 20\% & 7\ A < I \le 12.5\ A \\ At\ G = 10\% & 5\ A < I \le 7\ A \\ Otherwise & I = 0\ A \end{vmatrix} \tag{16}$$

where G is the gradient of the road in percentage (%), $a(t)$ is the instantaneous acceleration of the vehicle in m/s^2. Total length of wire can be computed as follows:

$$\begin{aligned} I_{wire} &= \pi \times \frac{h_2 - h_1}{2} \times \frac{L_{solenoid}}{d_w} \times \frac{h_2 - h_1}{2d_w} \\ I_{wire} &= \pi \frac{L_{solenoid}\left(h_2^2 - h_1^2\right)}{4d_w^2} \end{aligned} \tag{17}$$

where h_2 and h_1 is largest and smallest diameter of the solenoid respectively. d_w is the wire diameter and $L_{solenoid}$ is the length of the solenoid. Again

$$R = \frac{4\rho l_{wire}}{\pi d_w^2} \tag{18}$$

where R is the wire resistance in Ω, ρ is the resistivity of conductor in Ωm, l_{wire} is the total length of the conductor and d_w is the wire diameter. In combine equations (17) and (18) can be written as:

$$d_w = \sqrt[4]{\frac{\rho L_{solenoid}\left(h_2^2 - h_1^2\right)}{R}} \tag{19}$$

where d_w is the diameter of the coil, mm.

Figure 4 A laboratory scale-EMA for CVT operation (see online version for colours)

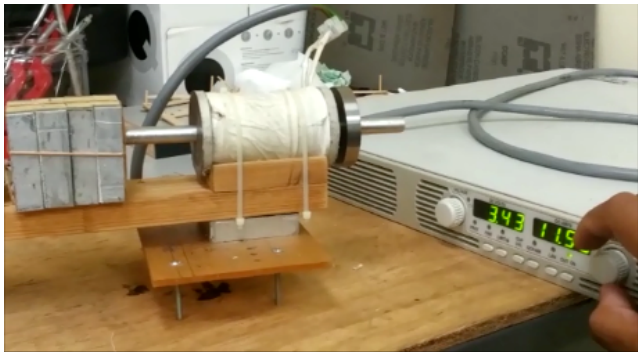

A laboratory scale EMA has been developed as shown in Figure 4. The core objective of this laboratory scale metal bobbin was to used for parametric study of the EMA which will help to optimise the design of full-scale EMA-CVT for passenger car.

The bobbin is made with cast iron and coiling on its with copper wire to increase the electric energy density (E_{em}) and result in stronger electromagnetic force. A non-magnetic (aluminium alloy) piston is attached with a stopper or mover, which acts as an object of actuating the movable sheave of the pulley. The objective of the laboratory scale EMA

has been made is to study the actuation characteristics of the full-scale EMA-CVT of passenger car. In preliminary experiment, a 10 A current has supplied to move the 5 N object on the wood surface and 5 A to move the 5 N object on the normal road surface.

Table 1 Specification of the lab scale EMA

Parameters	*Values*
Wire diameter (d_w)	0.00145 m
Length of actuator (L)	0.065 m
Actuator min. diameter (h_1)	0.030 m
Actuator max. diameter (h_2)	0.050 m
Packing factor = Actual winding / theoretical winding	105/200 = 0.525
Number of turns (N) = $\frac{L(h_2 - h_1)}{2d_w^2} \times packing\ factor$	163 turns

Friction coefficient of the aluminium load and wood surface was considered 1 while on normal road surface it was 0.4. The actuation time of the load was recorded as 3.5 s on the wooden surface and 2.8 s on the normal road surface. The acceleration time are considered as the vehicle acceleration time to reach the speed of 0–100 km/h. Table 1 shows the specification of the small-scale EMA.

3 EMA-CVT development

The EMA (Figure 5) has been developed with 3000 number of wire turns onto the steel bobbin of solenoid length 220 mm, which is capable to produce the electromagnetic force of 200 N to 300 N with supplied current of 5.16 to 6.23 A, respectively. The hollow bobbin has been made with steel for the stronger electromagnetic force generation. It functions to hold the copper coil, attract the iron disk with its strong electromagnetic field and actuate the movable sheave of the secondary pulley. The full scale EMA specification is shown in Table 2.

Figure 5 EMA-CVT for passenger car, (a) EMA (b) EMA with spring (see online version for colours)

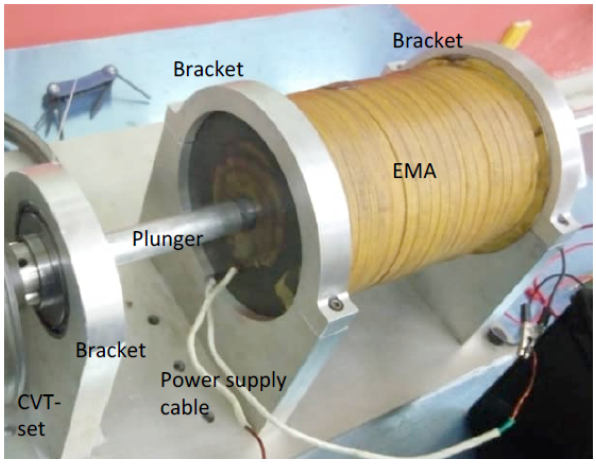

3.1 Power system

Using the lithium ion ($LiFePO_4$) battery cells, the power system of the EMA has been built. The each cell of the battery of power pack nominal voltage is 3.5 V and capacity is 43 Ah. The module has been built with two (2) cells in series and two in parallel for nominal voltage of 7 V and capacity of 86 Ah. Thus getting the 50 V and 86 Ah, seven modules are connected in series. The battery can be charged and discharged in shortly to avoid the power interruption of the EMA.

Table 2 Specification of the EMA winding for full-scale actuator

Coil diameter (d_w), mm	1.63
Length of solenoid ($L_{solenoid}$), m	0.22
Outer diameter 1 (D_2), mm	190
Inner diameter 2 (D_1), mm	80
Packing factor: $R_f = \frac{105(actualwinding)}{200(theoreticalwinding)}$	0.525 (based on lab scale)
Number of turns (N) = $\frac{L_{solenoid}\left(D_2 - D_2\right)}{2d_w^2} \times packingfactor$	2,420 *turns*
Length of coil (L_w) = $\pi \frac{L_{solenoid}\left(D_2^2 - D_1^2\right)}{4d_w^2} \times packingfactor, m$	1,26
Effective area $A_e = \pi\left(\frac{D_2^2 - D_1^2}{4}\right)m^2$	0.00454

3.2 Pulley and belt modification

The metal push V-belt is considered to use in the Intelligent EMA-CVT, which has overcome the problems that have in the rubber belt pulley such as slips and transmission loses. The metal push V-belt and pulley that used by the Toyota Wish CVT Specifications (2018) which has been customised for PROTON PREVE car. The two different shifting behaviours of the metal belt CVT has been considered. The first mode is the creep mode. This mode has been characterised based on the ratio of the clamping force acting on the primary pulley to that acting on the secondary pulley. The intelligent EMA-CVT influences the creep mode rate of speed ratio and the tangential velocity.

3.3 IoT-based control system development

The functional block diagram of the EMA for continuously variable transmission (EMA-CVT) is shown in Figure 6. The power supply system of the EMA has been made by using a 50 V and 43 Ah capacity $LiFePO_4$ battery, which is controlled by FLC to set the targeted CVT gear ratio. The EMA develops the electromagnetic force which is always more than the clamping force of the CVT's pulley in order to set the gear ratio $1.2 < GR \leq 6.5$. The speed sensor and slope sensor has been accumulated to control the power supply to the EMA.

Based on the error, the different between and targeted and actual ratio, the FLC makes appropriate adjustments of the CVT by controlling the power supply to the EMA. In order to adjust the targeted gear ratio of the CVT, the movable sheave of the primary and secondary pulleys position has been changed by the EMA actuating force. There is a failsafe mode built into the CVT to prevent damage in case some of the sensors malfunction. During failsafe mode, shifting to manual mode for fixing the gear ratio equivalent to first gear and to save the CVT from damage a central manual switching system (CMSS) has been used.

Figure 6 Functional block diagram of i-EMA-CVT (see online version for colours)

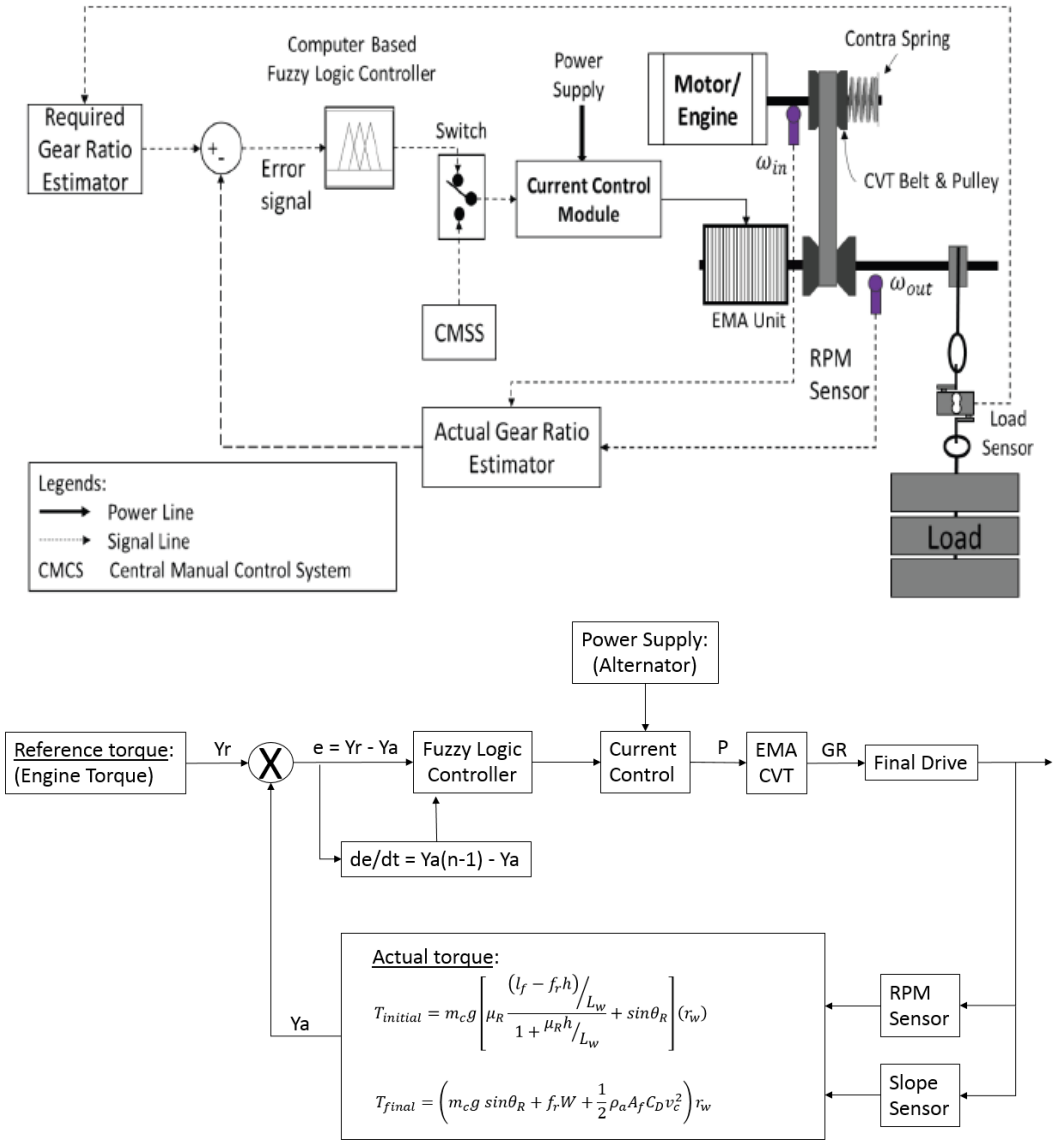

Block diagram of the intelligent EMA-CVT control system has been developed based on the actuation of the pulleys sheaves to maintain the transmission ratio for the vehicle either in acceleration or cruising. Continuously, a computer-based controller will collect the actual data of wheel speeds and vehicle slopes from sensors, and calculate the real

torque of the car for different driving modes (denotes as Y_a). With reference to the engine torque (denotes as Y_r), the torque error is calculated, $e_T = Y_r - Y_a$ for the instantaneous operational mode. The torque error (e_T) and its derivation (RTE = de/dt) main input to the FLC to estimates a proper current or power (P) to operate the EMA to yield a suitable GR for driving the car. Based on the signal from FLC, current control acts as a gate to allow proper amount of current from alternator to the EMA solenoid. With this current, the plunger or movable sheave position is controlled. The alternator is attached to the rotating engine to produce the energy for the EMA.

The functional block diagram has been develop to control the operation of the EMA to actuate the CVT. The system works based on two modes; automatic mode and manual modes. Manual mode or failsafe mode was introduced to prevent damage to the transmission parts in case some of the sensors malfunction. During failsafe mode, the driver will shift the CMSS to set the gear ratio equivalent to first gear.

During automatic mode, different set of load weights was used to mimic the car traction torque and gear ratio requirement for various road conditions. Bending beam load cell using strain-gauge-based technology was used to measure weight and convert it into electrical signal. The computer-based controller then converts the signal into an equivalent transmission torque as well as the required gear ratio value. At the same time, the controller continuously collects the real-time reading of motor and transmission shaft speeds to estimate the actual gear ratio of the system. Based on the error signal between the actual and required gear ratio, a proper signal is produced by FLC to the digital control switching system (DCSS) to allow a proper current flow to the EMA to generate clamping force at movable sheave.

3.4 Fuzzy logic approach

Approach of fuzzy logic is for predicting of performance as well as dynamic behaviour of EMA-CVT system over time. EMA actuation control systems with FLC exercises desired electromagnetic force thus minimise power consumption. The control system of the EMA is structured with controlled variable and regulated variable based on the study (Richard et al., 2019; Sreenatha et al., 2004; Hossain and Rahman, 2011).

Figure 7 Fuzzification model for the EMA-CVT system (see online version for colours)

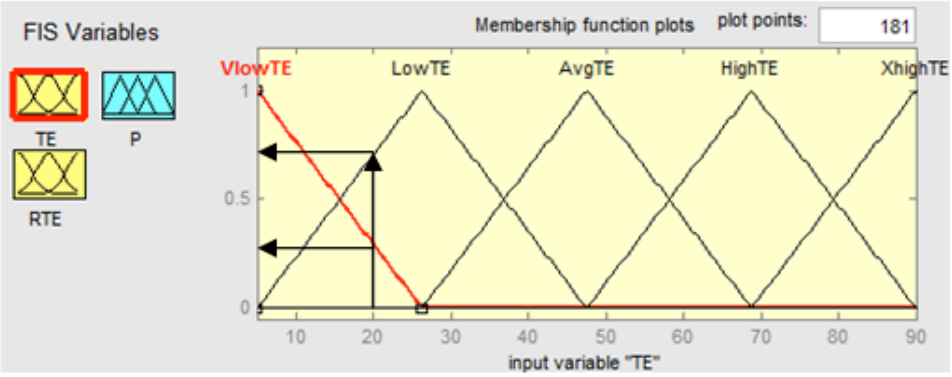

In this study, the variable for the fuzzy logic simulation is considered to include torque error (TE), variable torque error (RTE) and controlled variable as electricity consumption

(P). It is stated that the values of the member actions (RTE) change their values over time. For example, TE changes from 5 to 90 Nm, RTE fluctuates from –5 to 5 Nm/s, and *P* is measured from 50 to 200 watt. For example, at *TE* = 5; it is certain that the torque error is 'very low (Vlow)', and as the value of TE moves toward 26.25 it is become less certain that it is 'Vlow' and more certain that it is 'Low' as shown in Figure 7.

Table 3 represents the membership function associated with the linguistic value like 'Vlow' and a similar notation for others. Now to illustrate the fuzzification process, linguistic expressions and membership functions of torque error (*TE*) which are simulated based on equations (20)–(22).

Table 3 Coefficients of membership functions for FIS parameter of TE

Linguistic variables	*Type*	*Coefficient (Nm)*		
		c_1	c_2	c_3
VLow-TE	Z-shaped	5	26.25	-
Low-TE	Triangular	5	26.25	47.5
Average-TE	Triangular	26.25	47.5	68.75
High-TE	Triangular	47.5	68.75	90
XHigh-TE	S-shaped	68.75	90	

To comprehend fuzzification, an example is considered. It is assumed that at a particular point at time *t*, *TE*(*t*) = 20 Nm and *RTE* = 2.5 Nm/s. *TE*(*t*) indicates the system input and it has its membership function truth values that can be computed of based on fuzzy inputs from fuzzy logic expert system:

$$\mu_{Vlow}(TE(t)) = \begin{cases} 1; & (TE) \le 5 \\ \dfrac{26.25-(TE)}{21.25}; & 5 < (TE) < 26.25 \\ 0; & (TE) \le 26.25 \end{cases} \tag{20}$$

$$\mu_{Low}(TE(t)) = \begin{cases} 0; & (TE) \le 5 \\ \dfrac{(TE)-5}{21.25}; & 5 < (TE) \le 26.25 \\ \dfrac{47.5-(TE)}{21.25}; & 26.25 < (TE) < 47.5 \\ 0; & (TE) \ge 47.5 \end{cases} \tag{21}$$

$$\mu_{Pos}(RTE(t)) = \begin{cases} 0; & (RTE) \le 1 \\ \dfrac{(RTE)-1}{2}; & 1 < (RTE) \le 3 \\ \dfrac{5-(RTE)}{2}; & 3 < (RTE) < 5 \\ 0; & (RTE) \ge 5 \end{cases} \tag{22}$$

Figure 8(b) shows the instrumentation system for the EMA testing with the Toyota Wish CVT Specifications (2018), load cell, rpm sensor, a battery pack (50 V, 100 Ah) and electromagnetic force monitoring laptop. The test-bed was built on a strong table with a

thick wooden top and was reinforced with one-centimetre-thick aluminium plate. The main frame with dimension 180 cm × 80 cm is made by thick hollow steel to ensure its steadiness. The CVT set was mounted at place with one and half inch aluminium bar and was fixed at the table top with bolt from below. All the associated original bearings were used to ensure the precise and smooth movement of the movable sheave of the primary and secondary pulleys. Moreover, to ensure a better preciseness of the test-bed, all the mounting holes were made with the CNC milling machine. The driver side of the CVT was connected to the AC traction motor while the driven one was connected to the propeller shaft. On the other side of the driven pulley the EMA was placed. The EMA function is to control the position of the movable sheave of the pulley by moving the plunger back and forth.

Figure 8 (a) Electromagnetic CVT testing and (b) Instrumentation system of EMA for the CVT operation (see online version for colours)

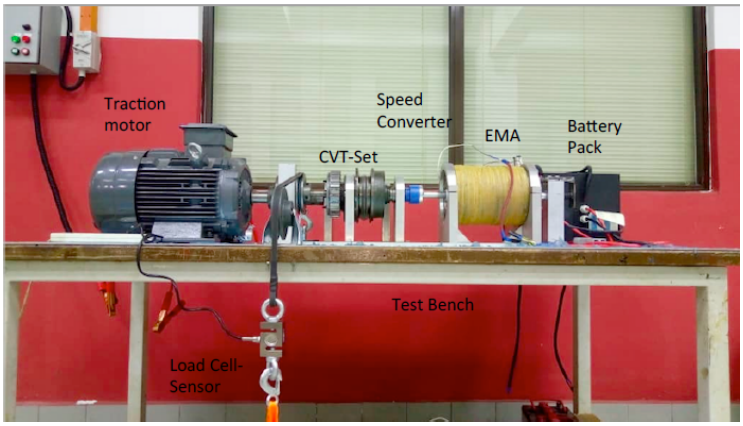

(a)

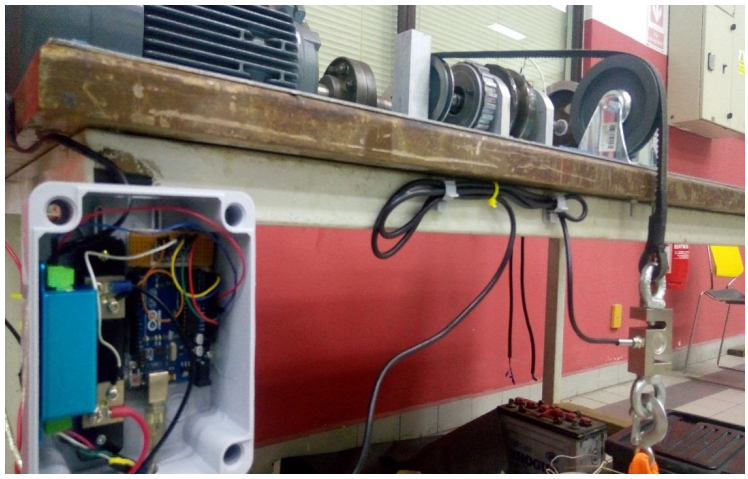

(b)

Furthermore, to propel the CVT system an AC traction motor was selected. Torque to propel the CVT needed to be delivered from the electric motor can be calculated by using pulley gear ratio and torque in secondary transmission shaft. The transmission torque at the propeller was found by dividing the traction torque at wheel by the final drive ratio. The load cell and rpm sensors are connected with fuzzy controller to control the power

flow to the EMA. An equivalent torque at propeller shaft was estimated and created by attaching a hanging load as in a Prony-brake dynamometer. Dynamometer is a device for measuring mechanical power transmitted by a rotating shaft. Since power is the product of torque (turning force) and angular speed, dynamometers are essentially torque-measuring devices. A Prony-brake develops mechanical friction on the periphery of a rotating pulley by means of brake blocks that are squeezed against the wheel by tightening the bolts until the friction torque FR balances the torque WL. Based on equation, $m = Tp/\ gl$ the hanging mass 58 kg required to create torque of 228 Nm at propeller shaft for mimicking a 1600 kg car cruising at 120 km/h (33.33 m/s) speed at the slope of 11.3 degree. So that by using 58 kg load hanging at the brake hand, 228 Nm torque was created at the propeller shaft. At the same time, the hanging load was measured by the load cell and become an input signal for the FLC.

4 Performance of EMA-CVT prototype

The experiment has been set as shown in Figure 8(a). The AC motor, the fixture of CVT fixings, CVT system including the EMA with plunger, spring, battery pack, digital load cells to measure the applied load in terms of voltage signal, fuzzy controller to control the power flow of the EMA to maintain the gear ration of the CVT and data logger. The optimum temperature of the EMA has been considered 35°C and current supplied has been limited to 3–4 A. The experiment has been conducted with the maximum current supplied of 4 A.

The EMA has a positive impact on the CVT car performance in terms of fast acceleration by fast actuation response and remarkable reduction of transmission loss. The EMA-CVT has advantages over manual, automatic and other existing CVT because of its less and light transmission unit. Experimental result shows that the acceleration time of the EMA-CVT (based on ¼ model) is 35% less than the hydraulic actuated CVT, 41% than the manual transmission and 52% than the automatic transmission.

The performance of EMA actuated CVT is investigated experimentally as shown in Figure 8(a). The EMA able to develop the electromagnetic forces 101.22 N to 274.82N as the clamping forces by supplying current in the range of 3–6 A with a 50 V battery (Figure 9). The EMA is able to develop the electromagnetic forces 101.22–274.82 N and dynamic torque 31.38–85.19 Nm at transmission gear ratio of 0.820–2.369.

Figure 9 Electromagnetic force vs. current to adjust the gear ratio (see online version for colours)

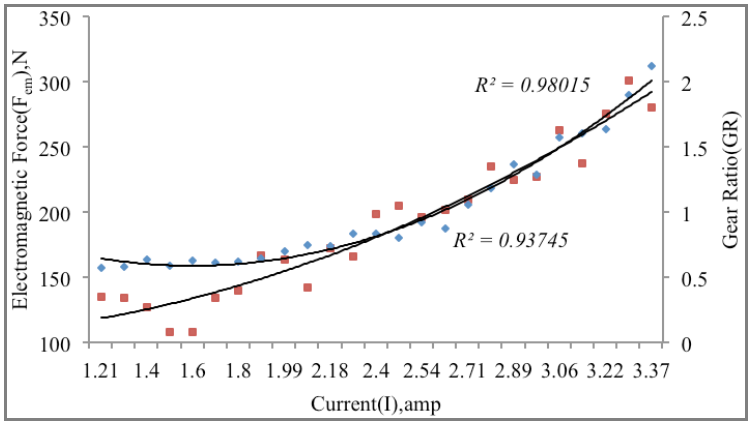

Figure 10 shows the pulleys rpm with different gear ratio of the CVT. The rpm of the secondary pulley has changed based on the actuation force of the secondary pulley which has been made with the EMA and a back spring of stiffness 5.86 N/mm. However, the primary pulley's actuation force has been with a spring of stiffness 11.72 N/mm.

Figure 10 RPM of the pulleys based on the gear ratio (see online version for colours)

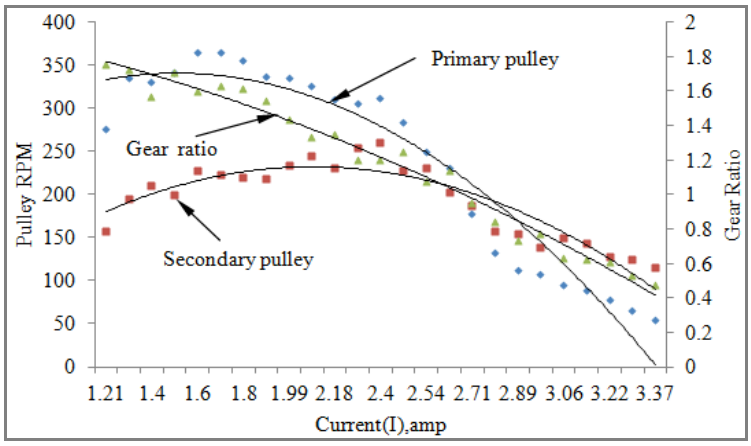

Figure 11 Heat generation of the EMA (see online version for colours)

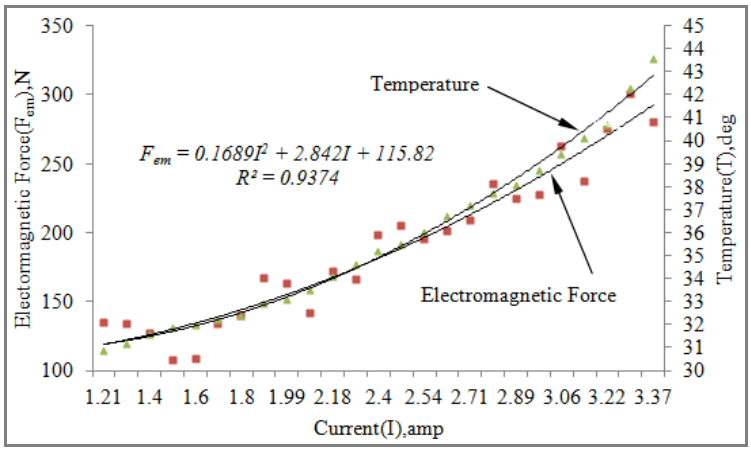

Heat generation of the solenoid has increased with increasing the current supply to the solenoid. Figure 11 shows the heat generation of the solenoid due to the supplied current. The resistivity of all elemental metals increases as temperature increases, the resistance of what the coil is wound increase and it gets hotter. It indicates that with a fixed number of turns and a fixed voltage driving the coil, the current (I) through it decrease as increase the temperature, weakening the strength of the magnetic, $H = NI$. The resistivity of the coil due to heat development can be estimated as:

$$\rho = \rho_0(1+\alpha\Delta T) \text{ or } R = R_0(1+\alpha\Delta T)$$

$$\text{as } R = \frac{\rho A}{L}$$

where ρ_0 is the original resistivity and α is the temperature coefficient of resistivity. The temperature coefficient of resistivity α of copper coil 3.91×10^{-3} per degree Celsius.

Figure 12 CVT's pulley rpm and gear with supply current (see online version for colours)

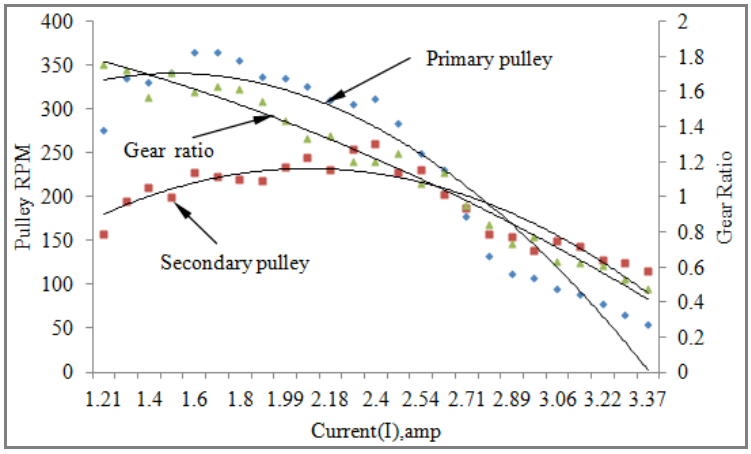

Figure 13 Response of the pulley to adjust the gear ratio (see online version for colours)

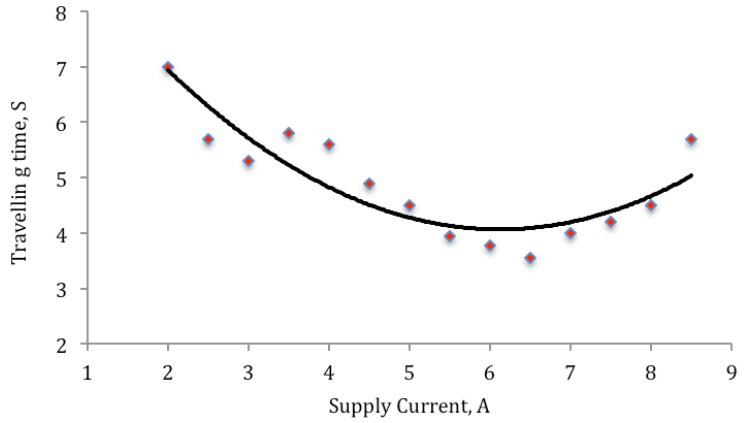

Figure 14 Travelling time of the movable sheave for the desired gear ratio (see online version for colours)

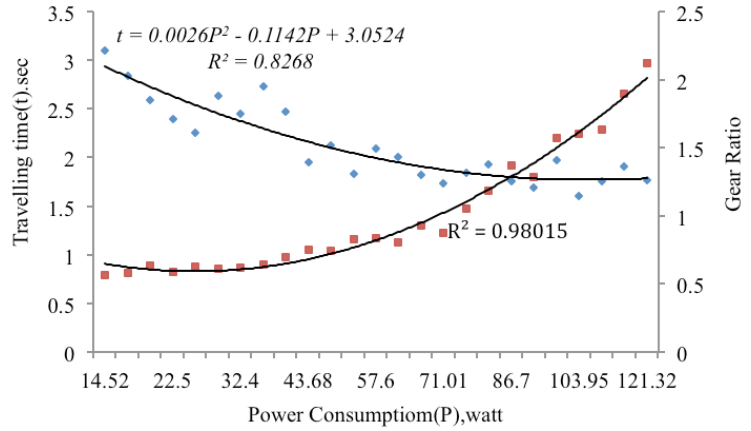

Figure 12 shows the changing of the pulleys RPM with changing the gear ratio. The solenoid able to push the movable sheave of the pulley with plunger in the desired distance when current supply in the range of 2–5 A. While, it is different when the current supply to the EMA is less than 3 A. The responding time of the plunger of the EMA in free loaded is less compared to with payload of 40 kg. This is could be the slip associated of the belt with the pulley's surface.

The performance of the EMA-CVT has found very high when the current supplied was in the range of 3–4 A with out cooling fin and 5–6 A with fin. However, its performance has decreased drastically with changes the current supplied in the range of 6–8 A (Figure 13). The maximum temperature was recorded 50°C at the current supplied 8 A.

Figure 14 travelling time of the plunger is in the range of 1.8–3.1 s without loading. It shows higher with the incremental loads higher the travelling time. However, prime mover was unable to transmit torque when the pay-load increased more than 50 kg.

Figure 15 Output torque comparison (see online version for colours)

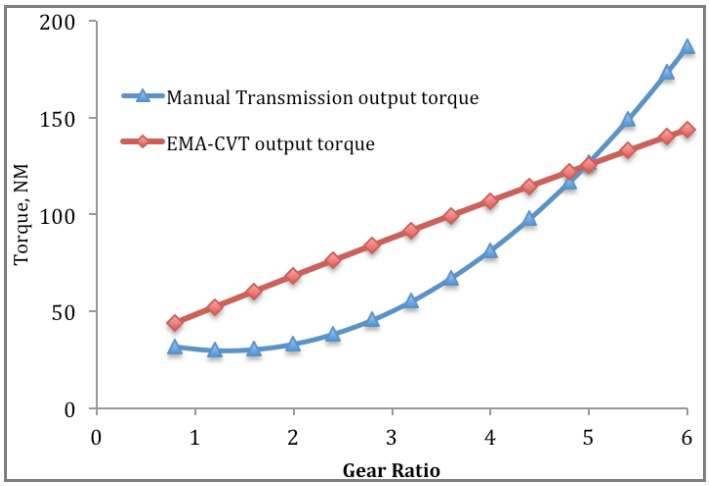

Figure 16 Fuzzy simulated model validation (see online version for colours)

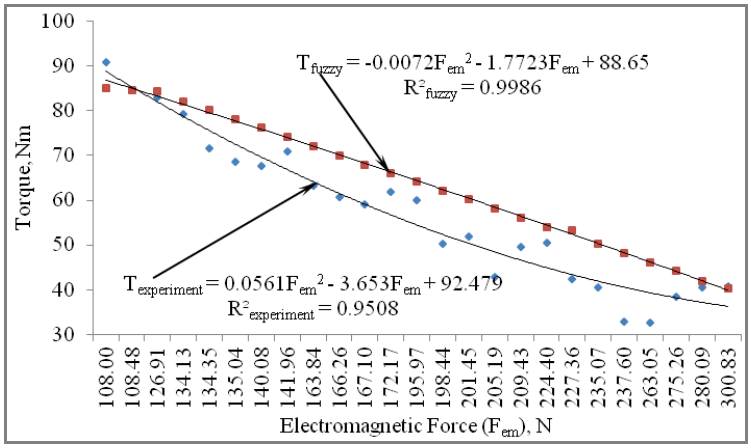

Figure 15 shows the wheel torque of the vehicle which has been made with considering the final drive ratio 4:1. Wheel torque has calculated as $T_w = T_{in(CVT)}x\ Ng\ x\ N_D(1 - i_{cvt})$ or $T_{out(CVT)}x\ N_D$ where, T_w is the wheel torque, Ng adjusted gear ratio of the CVT, N_d final drive ratio, i_{cvt} slippage of the CVT belt over the pulleys sheave surface, $T_{out(CVT)}$ output torque of the CVT. The $T_{out(CVT)}$ was found very low due to the excessive slip of the belt over the pulleys sheave surface. However, it is found in better mode when the gear ratio is higher and CVT is operated with free load.

Figure 16 shows the validation of the fuzzy simulation model with the EMA-CVT experimental result. The correlations between measured (experimental) and predicted (FLES) values of traction torque have found 90.99%, which closely verify the fuzzy simulation model. However, the mean relative error of measured and predicted values from the FLES model on traction torque is found as 4.0% since this study neglecting transmission losses.

5 EMA-CVT deliverables

The full-scale EMA-CVT ensures gear ratios for reduction, cruising and reverse without making rattling noise which is concluded with the EMA-CVT test-rig result. Furthermore, the EMA-CVT ensures the uniform power transmission in slope climbing and accelerate the car in 5 to 7 sec which has been made by applying the payload (Payload = $W\sin\theta$). It reduces the power transmission losses about 75% and save engine power consumption about 20% and make the vehicle energy efficient. However, road-test required to valid the test-rig result.

The prototype's CMSS ensures the EMA operation with actuating the CVT system in case of IOT-based system failure.

6 Benefits of the EMA-CVT

The full scale prototype 'intelligent electromagnetic CVT' has been developed and tested. The prototype EMA-CVT improves the vehicle transmission loss by 80% with accelerating the car in 5–6 sec. Therefore; the EMA-CVT contributes to reduce the emission level. The mass selling of EMA-CVT will enhance to consolidate a new industry where could be 200–300 new jobs created. Based on the performance of the EMA-CVT, it could be claimed that 15% less fuel consumption for the CVT transmission than with a manual transmission along with a reduction in harmful emissions of about 30%.

7 Conclusions and recommendation

7.1 Conclusions

This paper present theoretical and experimental work on the EMA and its feasibility for implementation in CVT. On the basis of electromagnetic force of the EMA and clamping force, mathematical equations are established for simulating the EMA-CVT system response. The main conclusions drawn from this study are as follows:

- The full-scale EMA is able to develop electromagnetic forces in the range of 400 N to 500 N equivalent to the clamping forces by supplying current in the range of 4.8–5.4 A. This is optimised with the development of a laboratory scale EMA number of copper coil turns 163 which is able to develop electromagnetic force in the range of 0.5 N to 44.33 N by supplying current up to 10.50 A.
- The performance of the full-scale EMA shows dictates that it would be able to actuate the CVT pulleys to set the correct gear ratio as required of the vehicle traction. However, the potentiality of the EMA-CVT needs to be validated with the road test result.
- Ohmic heat development of the EMA severally effects the EMA response to adjust the gear ratio. By using the liquid cooling tubes around the EMA the ohmic heat development can be avoided.

7.2 Recommendation

The EMA should be covered with an aluminium alloy plate and polypropylene to prevent the electromagnetic compatibility (EMC). While, the glycol liquid cooling of EMA can avoid the ohmic heating effect and reduces the power losses.

Acknowledgements

The authors are grateful to the Ministry of Higher Education Malaysia for financing this project with Prototype Research Grant Scheme (PRGS16-004-0035) and Research Management Centre of IIUM for the grants 'Rig-Flagship' (Ref. IRF19-032-0032). The authors are also grateful to the technician for helping this project to develop the full scale prototype.

References

Ang, K.K., Quek, C. and Wahab, A. (2002) 'MCMAC-CVT: a novel on-line associative memory based CVT transmission control system', *Neural Networks*, Vol. 15, No. 2, pp.219–236.

Boldea, I. and Nasar, S.A. (1997) *Linear Electric Actuators and Generators*, 1st ed., Cambridge University Press, UK.

Brockbank, C. and Burtt, D. (2007) *Developments in Full Toroidal Traction Drive Infinitely and Continuously Variable Transmissions*, SAE Technical Paper 2007-01-3740.

Denton, T. (2011) *Automobile Mechanical and Electrical System*, Elsevier, Oxford.

Hossain, A. and Rahman, A. (2011) 'Fuzzy expert system for controlling the swamp vehicle intelligent air-cushion system', *International Journal of Automotive Technology*, Vol. 12, No. 4, pp.334–339, Springer Publication.

Hossain, A. and Rahman, A. (2011) 'Nonlinear control of an intelligent air-cushion system of swamp vehicle', *Proc. IMech E, Part D, Journal of Automobile Engineering*, Vol. 225, No. 6, pp.721–734.

Jaafar, A.H., Rahman, A., Mohiuddin, A.K.M. and Rashid, M. (2016) 'Modelling of an advanced charging system for electric vehicles', *Int. Conf. Mech. Automot. Aerosp. Engineering 2016*, Vol. 184, No. 1, p.012023.

Kelly, J. (2017) *CVT Transaxle Steel Push Belt Construction Weber State University*, Ogden, Utah, 84408, USA.

Kluger, M.A. and Fussner, D.R. (1997) 'An overview of current CVT mechanisms, forces and efficiencies', *Transmission and Driveline System Symposium 1997*; SAE Paper No. 970688, SAE SP-1241, pp.81–88.

Leander, W., Matsch, L. and Morgan, J.D. (1987) *Electromagnetic Electromechanical Machines*, 3rd ed., John Wiley & Sons, Canada.

Nissan (2017) *All New Teana*, Nissan Malaysia [online] https://www.nissan.com.my/vehicles/teana (accessed 30 March 2017).

Nissan Technological Development Activities Overview: Xtronic Cvt (2012) *Archived from the Original on 5 September* [online] http://Nissan-global.com (accessed 19 September 2009).

Nogill, P., Ryu, J.H. and Lee, H.W. (2009) 'Development of the inner spherical CVT for a motorcycle', *International Journal of Automotive Technology*, Vol. 10, No. 3, pp.341–346.

Pesgens, M., Vroemen, B., Stouten, B., Veldpaus, F. and Steinbuch, M. (2006) 'Control of a hydraulically actuated continuously variable transmission', *Vehicle System Dynamics*, Vol. 44, No. 5, pp.387–406.

Rahman, A., Hossain, A., Zahirulalam, A.H.M. and Mahbubur, R. (2012a) 'Fuzzy knowledge-based model for prediction of traction force of an electric golf car', *Journal of Terramechanic*s, Vol. 49, No. 1, pp.13–25, Elsevier Publisher.

Rahman, A., Sharif, S., Hossain, A., Mohiuddin, A.K.M. and Zahirul, A.H.M. (2012b) 'Kinematics and nonlinear control of an electromagnetic actuated CVT system for passenger vehicle', *Journal Mechanical Science and Technology*, Vol. 26, No. 7, pp.2189–2196.

Rahman, A., Afroz, R. and Alam, Z. (2014a) 'Development of electric vehicle: Public perception and attitude, the Malaysian approach', *World Review Intermodal Transportation Residence*, Vol. 5, No. 2, pp.149–167.

Rahman, A., Sharif, B.S., Mohiuddin, A.K.M., Rashid, M. and Hossain, A. (2014b) 'Energy efficient electromagnetic actuated CVT system', *J. Mech Sci Technol.*, Vol. 28, No. 4, pp.1153–1160.

Richard, F., James, K. and Gregory, L. (2019) *Electromagnetic Radiation*, Oxford University Press, Oxford, UK.

Sharif, B.S., Rahman, A., Mohiuddin, A.K.M. and Hossain, A. (2013) 'Study on the development of a fuzzy logic control electromagnetic actuated CVT system', *Int. J. Engineering Systems Modelling and Simulation*, Vol. 5, No. 4, pp.217–225.

Sreenatha, G.A., Choi, J.Y. and Wong, P.P. (2004) 'Design and implementation of fuzzy logic controller for wing rock', *International Journal of Control, Automation, and Systems*, Vol. 2, No. 4, pp.494–500.

Tanaka, H. and Machida, H. (1996) 'Half toroidal traction-drive continuously variable power transmission', *Journal of Engineering Tribology, IMechE*, Vol. 120, No. 1996, pp.205–212.

Tawi, K.B., Supriyo, S., Ariyono, S., Husain, N.A., Hamid, A.R.A., Azlan, M.A., Mazali, I.I. and Kob, M.S.C. (2015) 'Design of electro-mechanical dual acting pulley continuously variable transmission', *Journal of Mechanical Engineering and Sciences*, Vol. 8, No. 2015, pp.1332–1342.

Toshie, T (2004) 'Electromagnetic analysis coupled with motion for high speed circuit breakers of Eddy current repulsion using the tableau approach', *IEEJ Transaction Power Electronics*, Vol. 124, No. 6, pp.859–865.

Toshie, T. et al. (2004) 'An electromagnetically actuated vacuum circuit breaker developed by electromagnetic analysis coupled with motion', *IEEJ Transaction Power Electronics*, Vol. 124, No. 2, pp.321–326.

Toyota Wish CVT Specifications (2018) [online] https://www.stcars.sg/singaporecar/cars/toyota-wish-2677/specification (accessed July 2019).

Wong, J.Y. (2001) *Theory of Ground Vehicles*, 3rd ed., Vol. 1, John Wiley & Sons, Canada.

Nomenclature

A_f	Frontal area	h_1	Outer radius of bobbin
A_e	Electromagnetic core effective area	H	Magnetic field intensity or strength
B	Flux density	h	Height of centre gravity
C_D	Dag coefficient	J	Current density
D_2	Core inner diameter	L_{wb}	Wheel base
D_1	Core outer diameter	L_w	Length of coil
D_S	Secondary pulley diameter	L_{stroke}	Pulley sheave moving distance or stroke length
D_P	Primary pulley diameter	L_{bobbin}	Length of actuator's bobbin
d_g	Differential length of the electromagnetic gap	$l_{singlewinding}$	Length of single winding,
d_w	Wire diameter	l_{fr}	Distance from the front wheel to centre gravity
e	Electrical current error	M_{pt}	Peak value of the time response
$\dot{e}$	Rate of current error	m_c	Mass of a car
fv	Final value of the time response	N	Number of turns
$\Im$ or F_m	Magnetomotive force	N_S	Secondary pulley speed
f_r	Rolling motion resistance coefficient	N_P	Primary pulley speed
f_r	Coefficient of rolling motion resistance	N_{out}	Number of winding in the solenoid surface
F_{roll}	Rolling resistance of the tires	n_d	Final drive ratio
F_g	Gravitational force	n_t	Transmission performance
F_{em}	Electromagnetic force	$P_{req,max}$	Maximum required propulsion power
F_{RL}	Road load force	R	Pulley sheave radius
F_C	Clamping force	$R_{\min}$	Minimum pulley sheave radius
F_{AD}	Aerodynamic drag force	$R_{\max}$	Maximum pulley radius
h_2	Inner radius of bobbin	R_S	Radius of secondary pulley